The effect of an intense terahertz irradiation on magneto-miniband transport in semiconductor superlattices

2001 J. Phys.: Condens. Matter 13 6625

(http://iopscience.iop.org/0953-8984/13/31/304)

INSTITUTE OF PHYSICS PUBLISHING JOURNAL OF PHYSICS: CONDENSED MATTER
J. Phys.: Condens. Matter **13** (2001) 6625–6632 PII: S0953-8984(01)22505-3

The effect of an intense terahertz irradiation on magneto-miniband transport in semiconductor superlattices

F Q Yan[1] **and X L Lei**[1,2]

[1] State Key Laboratory of Functional Materials for Informatics, Shanghai Institute of Metallurgy, Chinese Academy of Sciences, 865 Changning Road, Shanghai 200050, China
[2] Department of Physics, Shanghai Jiao Tong University, 1954 Hua Shan Road, Shanghai 200030, China

Received 5 March 2001, in final form 12 June 2001
Published 19 July 2001
Online at stacks.iop.org/JPhysCM/13/6625

Abstract
We study the miniband conduction of electrons in GaAs-based superlattices under an intense terahertz field and a longitudinal magnetic field based on balance equations for THz-driven transport. The linear mobility with small direct-current fields and the drift velocity and the electron temperature at high electric fields are calculated, under the influence of an intense THz radiation, as functions of the magnetic field. Impurity, acoustic, and polar-optical-phonon scatterings are taken into account and as many as 31 Landau levels are included in the treatment. We find that in the linear case an intense THz field greatly changes the behaviour of the mobility versus the magnetic field, giving rise to multiphoton–magnetophonon resonance. In the nonlinear case, the irradiation of an intense THz field may eliminate the magnetic field quenching of the drift velocity, which shows up at a certain high strength of the magnetic field in the absence of the THz radiation.

1. Introduction

Electron transport of semiconductor systems under intense radiation fields of terahertz frequency has been the subject of many theoretical and experimental studies in the literature for the past few years [1–11]. It has been predicted recently that multiphoton–magnetophonon resonant peaks may show up in the magnetoresistance of a two-dimensional polar semiconductor subject to a dc magnetic field and a crossed THz radiation field [10]. For miniband transport of electrons in a polar-semiconductor-based superlattice with narrow bandwidth, Shu and Lei [12] pointed out a few years ago that quantized magnetic fields parallel to its growth axis may induce strong oscillation of the linear mobility and drastic change of the velocity-field behaviour when polar-optical-phonon scatterings are resonantly enhanced or forbidden due to Landau quantization of energy levels. In particular, when the gap between neighbouring Landau levels is large enough that the polar-optical-phonon scattering is forbidden, the peak drift velocity of the miniband conduction may become quite small due to a strongly enhanced electron temperature. Such a magnetic field quenching of miniband conduction has recently been observed experimentally in quasi-one-dimensional superlattices [13]. The purpose of this paper is to investigate the effect of an intense THz radiation on this interesting interplay between Landau quantization and polar-optical-phonon scattering, and try to find the possible multiphoton–magnetophonon resonance in the miniband transport of semiconductor superlattices.

2. Transport balance equations in a THz radiation field

We consider a model superlattice system which is formed by periodic potential wells and barriers of finite heights along the z-direction with period d and is subjected to a longitudinal magnetic field $\boldsymbol{B} = (0, 0, B)$ in the z-direction. The electron energy spectrum of the superlattice forms minibands in the longitudinal direction due to the periodic potential. In the superlattice layer (x–y plane), it is quantized into Landau levels due to the magnetic field. Assuming that the energy separation between the longitudinal lowest and second minibands is large enough that only the lowest miniband needs to be taken into account, the electron state can be described, in the Landau representation, by the quantum number n of the Landau level ($n = 0, 1, 2, \ldots$), the transverse wavevector k_x ($-\infty < k_x < \infty$), the longitudinal wavevector k_z ($-\pi/d < k_z \leqslant \pi/d$), and the spin index σ, with energy given by (neglecting the spin-related energy for simplicity)

$$\varepsilon_n(k_z) = \left(n + \frac{1}{2}\right)\omega_c + \varepsilon(k_z). \tag{1}$$

Here $\omega_c = |eB|/m$ is the cyclotron frequency and m is electron band effective mass in the x–y plane, and $\varepsilon(k_z)$ stands for the energy dispersion of the lowest superlattice miniband, which, under the tight-binding approximation, is given by

$$\varepsilon(k_z) = \frac{\Delta}{2}[1 - \cos(k_z d)] \tag{2}$$

where Δ is the miniband width. The electron-space wavefunction can be expressed as

$$\psi_{n,k_x,k_z}(x, y, z) = e^{ik_x x}\chi_{n,k_x}(y)\xi_{k_z}(z) \tag{3}$$

where $\xi_{k_z}(z)$ stands for the tight-binding Bloch function in the z-direction,

$$\chi_{n,k_x}(y) \equiv \left(\frac{1}{\pi l_B 2^n n!}\right)^{1/2} \exp\left[-\frac{(y - y_0)^2}{2l_B^2}\right] H_n\left(\frac{y - y_0}{l_B}\right) \tag{4}$$

in which $y_0 \equiv -\mathrm{sgn}(e)k_x/l_B{}^2$, e is the electron (carrier) charge, $l_B \equiv (|eB|)^{-1/2}$ is the magnetic length, and $H_n(x)$ is the harmonic function of order n.

When a uniform dc electric field $\boldsymbol{E}_0 = (0, 0, E_0)$ and a sinusoidal terahertz ac field of amplitude $\boldsymbol{E}_\omega = (0, 0, E_\omega)$ and frequency ω are applied along the z-direction, the time-dependent total electric field $\boldsymbol{E}(t) = (0, 0, E(t))$ is given by

$$E(t) = E_0 + E_\omega \sin(\omega t). \tag{5}$$

Under the influence of this periodic time-dependent electric field, the time-dependent steady transport state of the system with high electron density in the absence of the magnetic field can be described by a lattice momentum shift p_d and an electron temperature T_e, which are to be determined by a set of momentum- and energy-balance equations as given in reference [14]:

$$eE_0/m_z^* + A_i + A_p = 0 \tag{6}$$

$$eE_0 v_{\rm d} - W + S_{\rm p} = 0. \tag{7}$$

Here $v_{\rm d}$ is the average drift velocity, $1/m_z^*$ is the ensemble-averaged inverse effective mass along the z-direction, $A_{\rm i}$ and $A_{\rm p}$ are respectively the impurity- and phonon-induced frictional acceleration, W is the rate of energy transfer from the electron system to the phonon system due to electron–phonon interaction, and $S_{\rm p}$ is the rate of gain of energy of the electron system from the radiation field through the multiphoton absorption and emission processes. Their expressions were given in reference [14]. These equations are momentum- and energy-balance equations time-averaged over an interval longer than the period of the high-frequency field. They give a reasonable description of averaged transport quantities of the system under a strong irradiation when the period of the radiation field is shorter than the momentum relaxation time τ_m of the system [9, 14]. For a GaAs-based system, τ_m is generally of the order of 10^{-12} s, and we expect these equations to apply to radiation fields of frequency higher than 0.5 THz.

In the presence of a longitudinal magnetic field, the above balance-equation description is still valid. The effect of the magnetic field is to transversely confine the electrons inside a circle with radius of the order of a magnetic length $l_{\rm B}$ and to quantize the energy spectrum related to electron transverse motion. The momentum- and energy-balance equations remain the same (equations (6) and (7)), but the expressions for the corresponding quantities are now given by

$$v_{\rm d} = \frac{1}{\pi l_{\rm B}^2 N_{\rm s} n_z} \sum_{n,k_z} \frac{{\rm d}\varepsilon(k_z)}{{\rm d}k_z} f(\varepsilon_n(k_z - p_{\rm d}), T_{\rm e}) \tag{8}$$

$$1/m_z^* = \frac{1}{\pi l_{\rm B}^2 N_{\rm s} n_z} \sum_{n,k_z} \frac{{\rm d}^2\varepsilon(k_z)}{{\rm d}k_z^2} f(\varepsilon_n(k_z - p_{\rm d}), T_{\rm e}) \tag{9}$$

$$\begin{aligned} A_{\rm i} = \frac{n_{\rm i}}{2\pi l_{\rm B}^2 N_{\rm s} n_z} \sum_{s,s',\boldsymbol{q},k_z} |u(\boldsymbol{q})|^2 c_{ss'}(l_{\rm B}^2 q_\parallel^2/2)|g(q_z)|^2 \sum_{n=-\infty}^{\infty} J_n^2([v(k_z+q_z) - v(k_z)]e_\omega) \\ \times\, \delta(\varepsilon_{s'}(k_z+q_z) - \varepsilon_s(k_z) - n\omega)[v(k_z+q_z) - v(k_z)] \\ \times\, [f(\varepsilon_s(k_z - p_{\rm d}), T_{\rm e}) - f(\varepsilon_{s'}(k_z+q_z-p_{\rm d}), T_{\rm e})] \end{aligned} \tag{10}$$

and

$$\begin{aligned} A_{\rm p} = \frac{1}{\pi l_{\rm B}^2 N_{\rm s} n_z} \sum_{s,s',\boldsymbol{q},k_z} |M(\boldsymbol{q},\lambda)|^2 c_{ss'}(l_{\rm B}^2 q_\parallel^2/2)|g(q_z)|^2 \sum_{n=-\infty}^{\infty} J_n^2([v(k_z+q_z) - v(k_z)]e_\omega) \\ \times\, [v(k_z+q_z) - v(k_z)]\delta(\varepsilon_{s'}(k_z+q_z) - \varepsilon_s(k_z) + \Omega_{\boldsymbol{q}\lambda} - n\omega) \\ \times\, [f(\varepsilon_s(k_z - p_{\rm d}), T_{\rm e}) - f(\varepsilon_{s'}(k_z+q_z-p_{\rm d}), T_{\rm e})] \\ \times \left[n\left(\frac{\Omega_{\boldsymbol{q}\lambda}}{T}\right) - n\left(\frac{\varepsilon_s(k_z) - \varepsilon_{s'}(k_z+q_z)}{T_{\rm e}}\right)\right]. \end{aligned} \tag{11}$$

In these equations, $N_{\rm s} \equiv N/(n_z S)$ represents the electron sheet density per period (S denotes the area of the superlattice layer and n_z is the total number of periods of the whole superlattice), $u(\boldsymbol{q})$ is the 3D Fourier transform of the impurity potential, $M(\boldsymbol{q},\lambda)$ is the 3D plane-wave representation of the electron–phonon matrix element for phonons with wavevector $\boldsymbol{q} = (q_x, q_y, q_z)$ in branch λ, having frequency $\Omega_{\boldsymbol{q}\lambda}$. In addition, $g(q_z)$ and $c_{ss'}(l_{\rm B}^2 q_\parallel^2/2)$ ($q_\parallel^2 \equiv q_x^2 + q_y^2$) are form factors related to the longitudinal miniband wavefunction and the transverse Landau quantized wavefunction respectively [12]. Furthermore, $n(x) = ({\rm e}^x - 1)^{-1}$ is the Bose function, and $f(\varepsilon, T_{\rm e}) = (\exp[(\varepsilon - \mu)/T_{\rm e}] + 1)^{-1}$ is the Fermi distribution function at the electron temperature T_e, with μ being the chemical potential determined by the sheet density of electrons from the equation

$$1 = \frac{1}{\pi l_B^2 N_s n_z} \sum_{n,k_z} f(\varepsilon_n(k_z), T_e). \tag{12}$$

The expression for W can be obtained from the A_p-expression by replacing the factor $[v(k_z + q_z) - v(k_z)]$ on the right-hand side of equations (11) by $[\Omega_{q\lambda}]$, and the expression for S_p is obtained by from the expression for $A_i + A_p$ by replacing the factor $[v(k_z + q_z) - v(k_z)]$ on the right-hand sides of both equations (10) and (11) by $[n\omega]$. Note that the effect of the radiation field enters through the quantity

$$e_\omega \equiv eE_\omega/\omega^2 \tag{13}$$

which shows up in the expressions for A_i, A_p, W, and S_p.

3. The effect of an intense THz field on transport

Equations (6) and (7) allow us to calculate linear and nonlinear miniband transport properties of semiconductor superlattices under the influence of a strong longitudinal magnetic field and an intense THz electric field. As an example, we consider a GaAs-based quantum-well superlattice having period $d = 9.0$ nm, well width $a = 6.0$ nm, miniband width $\Delta = 8.5$ meV, and electron sheet density $N_s = 2.0 \times 10^{14}$ m^{-2} per period. We use randomly distributed background impurities to mimic the overall elastic scattering and assume that the impurity density $n_i = 1 \times 10^{21}$ m^{-3}. For phonon scattering we take into account both longitudinal and transverse acoustic phonons, in addition to the longitudinal-optical (LO) phonons.

In the absence of the THz field, the calculated linear mobility at lattice temperature $T = 300$ K as a function of the strength of the magnetic field is shown as the solid line in figure 1, which is essentially the same as that plotted in figure 1 of reference [12], exhibiting strong mobility oscillation. As pointed out in reference [12], the mobility minima at $B \simeq 7$, 10.5, and 21 T, can be explained by the maxima in the density of states at the bottom and top of each separate Landau miniband under the quantizing magnetic field. When the magnetophonon resonance condition

$$M\omega_c = \omega_{LO} \tag{14}$$

$(M = 1, 2, 3, \ldots)$ is satisfied, final states exist for all electrons in the miniband to scatter to if they absorb an optical phonon, resulting in a larger magnetoresistance. The three minima just correspond to the cases with $M = 1$, 2, and 3 of the resonance condition.

Such an oscillation behaviour will be drastically affected when the superlattice is exposed to a radiation field of THz frequency. The dashed line and chain line in figure 1 are the linear mobility of the same superlattice subjected to a radiation field of frequency $\omega/2\pi = 1$ THz, having strength $E_\omega = 5$ and 10 kV cm^{-1} respectively. It is expected that some kind of resonance may appear around where the condition ($M = 1, 2, \ldots$ and $n = 0, \pm1, \pm2, \ldots$)

$$M\omega_c + n\omega = \Omega_{LO} \tag{15}$$

is approximately satisfied. This is indeed the case, as shown, for instance, by the $E_\omega = 5$ kV cm^{-1} curve. We can see that, in addition to the minima around the resonant magnetic fields in the absence of the THz radiation, which are identified by one integer $(M, 0)$ $(M = 1, 2, \ldots)$, there appear two new minima around $B = 18$ and 24 T, which can be identified by two integers (M, n) as (1, 1) and (1, −1), and another two new minima around $B = 8.6$ and 11.6 T, which can be identified as (2, 1) and (2, −1). However, due to the finite width of the Landau miniband,

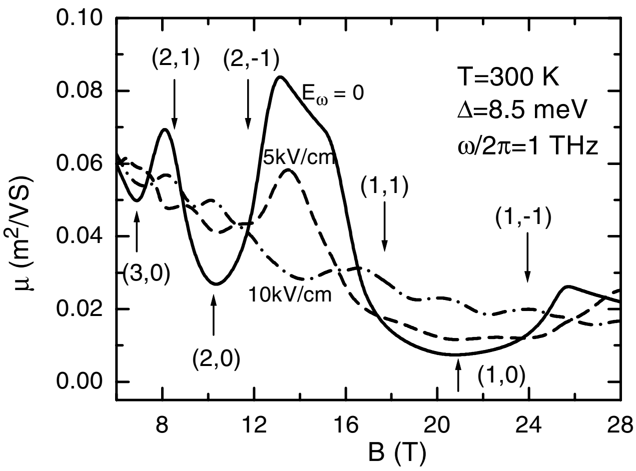

Figure 1. The linear (low-electric-field) mobility is shown as a function of the longitudinal magnetic field B for a GaAs-based superlattice having miniband width $\Delta = 8.5$ meV at lattice temperature $T = 300$ K, in the absence (solid curve) of a THz field and in the presence of a 1 THz high-frequency field, with strengths $E_\omega = 5$ and 10 kV cm^{-1}.

the resonant peaks are not so sharp as in the case of the two-dimensional electron gas [10]. Nevertheless, in comparison with that without a high-frequency field, the THz irradiation enhances the mobility around the magnetic field at which mobility minima locate in the absence of the radiation field. This trend remains true in the case of $E_\omega = 10$ kV cm^{-1} irradiation: the mobility around the resonant magnetic field continues to increase. The multiphoton peaks, however, are further smeared and barely seen.

In figure 2(a) we plot the calculated nonlinear drift velocity $v_{\rm d}$ as a function of the dc electric field E_0 for the same superlattice as discussed in relation to figure 1 ($\Delta = 8.5$ meV) at lattice temperature $T = 150$ K, in the absence and in the presence of a longitudinal magnetic field, for strengths $B = 11$, 15, 22, 25, and 30 T. These curves are similar to those calculated in reference [12] for a similar superlattice with a different strength of impurity scattering. As pointed out there, in view of the prohibition of the LO-phonon scattering, in the case without a radiation field, the $B = 30$ T and $B = 15$ T curves are distinctively different from the other four. There are two possible cases in which the LO-phonon scattering is forbidden. One is when the magnetic field is large enough that electrons can never jump to the higher Landau miniband by absorbing a LO phonon: $\omega_{\rm c} > \Omega_{\rm LO} + \Delta$. The other case can appear when the magnetic field satisfies the conditions $\omega_{\rm c} > 2\Delta$ and $n\omega_{\rm c} + \Delta < \Omega_{\rm LO} < (n+1)\omega_{\rm c} - \Delta$, such that the whole range of the electron energy in a miniband, after absorbing an LO phonon, will completely fall inside the gap between two neighbouring Landau minibands. Since acoustic phonons are far less efficient in dissipating energy from the carrier system, the electron temperature rises rapidly with increasing electric field. This quick rise of the electron temperature greatly limits the maximum average drift velocity of the carrier in this narrow miniband, and thus the peak drift velocity $v_{\rm p}$ is reached at a small critical electric field $E_{\rm c}$. $B = 30$ T and $B = 15$ T correspond respectively to the first and the second cases of the prohibition of the LO-phonon scattering. An intense radiation field at THz frequency has a drastic influence on the $v_{\rm d}$–E_0 behaviour. As shown in figure 2(b), when an ac field of frequency $\omega/2\pi = 1$ THz and amplitude $E_\omega = 5$ kV cm^{-1} is applied to the system, each $v_{\rm d}$–E_0 curve for nonzero magnetic field differs remarkably from the corresponding one without the THz field. The

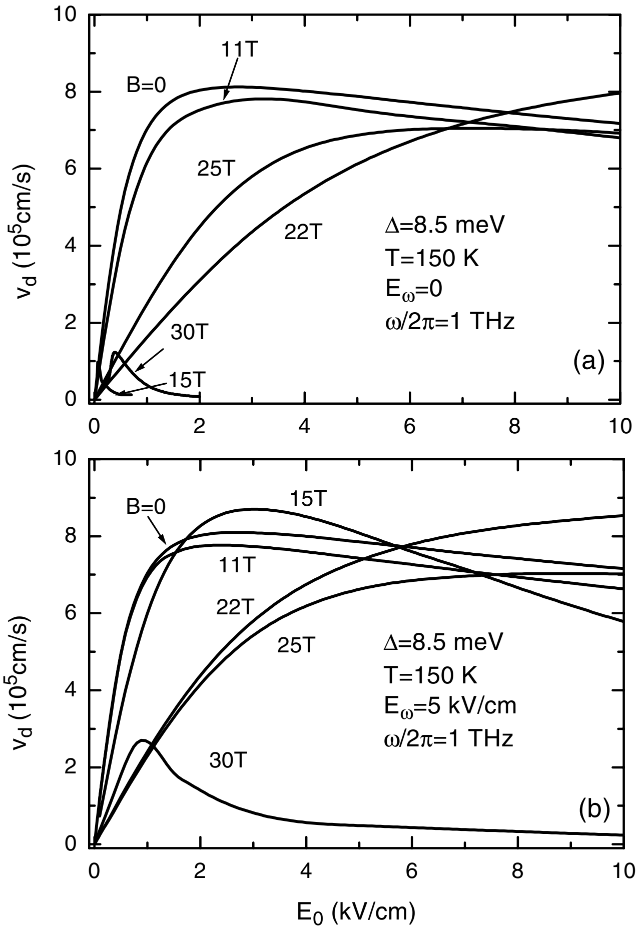

Figure 2. The nonlinear drift velocity $v_{\rm d}$ is plotted as a function of the dc electric field E_0 for the same superlattice as discussed in relation to figure 1 at lattice temperature $T = 150$ K subject to a longitudinal magnetic field, with strengths $B = 0$, 11, 15, 22, 25, and 30 T, in the absence of the THz field (a), and in the presence (b) of an intense radiation field of frequency $\omega/2\pi = 1$ THz and amplitude $E_\omega = 5$ kV cm^{-1}.

most dramatic changes are for the $B = 15$ T and $B = 30$ T curves: the magnetic field quenching of the drift velocity showing up previously in the absence of a high-frequency field disappears almost completely. On the other hand, in the case of zero magnetic field, where LO-phonon scattering can always take place through intra-miniband transverse transition, the effect of such a longitudinal THz radiation on the conduction of this narrow miniband is quite small. A strong magnetic field quantizes the transverse energy of the electron, leading to the alternating appearance of permitted/forbidden transitions between Landau minibands of LO phonons. When an intense THz field applies, the forbidden LO scatterings become available due to multiphoton-assisted processes.

For a superlattice with miniband width $\Delta = 12.1$ meV, the second condition for LO-phonon scattering prohibition cannot be satisfied. The magnetic field quenching of the drift velocity in the absence of the high-frequency field occurs only at the highest magnetic field (around $B = 30$ T). The mobility at low dc electric field decreases with increasing magnetic

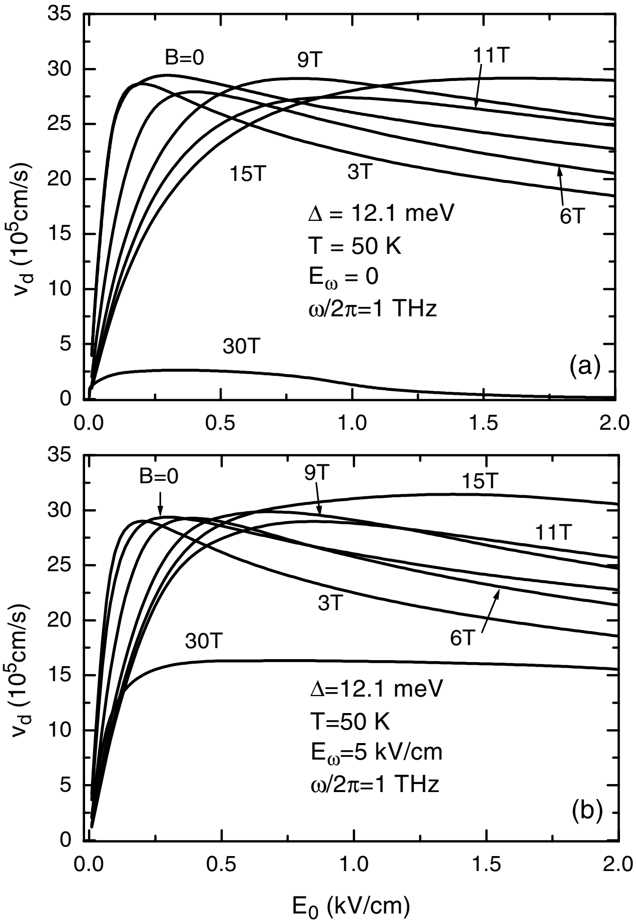

Figure 3. The nonlinear drift velocity v_d is plotted as a function of the dc electric field E_0 for another GaAs-based superlattice having miniband width $\Delta = 12.1$ meV at lattice temperature $T = 50$ K subject to a longitudinal magnetic field, with strengths $B = 0$, 3, 6, 9, 11, 15, and 30 T, in the absence of the THz field (a), and in the presence (b) of an intense radiation field of frequency $\omega/2\pi = 1$ THz and amplitude $E_\omega = 5$ kV cm^{-1}.

field up to $B = 15$ T, as shown in figure 3(a). This is in qualitative agreement with the experimental observation [13]. The application of an intense high-frequency field (frequency $\omega/2\pi = 1$ THz, amplitude $E_\omega = 5$ kV cm^{-1}) changes the v_d–E_0 behaviour greatly, with the most remarkable effect showing up in the $B = 30$ T curve.

4. Conclusions

We have analysed linear and nonlinear miniband transport of electrons in polar-semiconductor-(GaAs-) based superlattices under a quantized magnetic field and an intense THz electric field, by means of nonparabolic balance equations for THz-driven transport extended to include the Landau quantization due to a magnetic field. We find that the main effect of an intense THz radiation comes from the role of multiple-photon processes, which, in the linear case, introduce multiphoton resonances into otherwise typical magnetophonon resonant behaviour of the mobility as a function of the magnetic field. In the nonlinear case, the multiphoton processes release the condition for LO-phonon scattering prohibition and thus eliminate the magnetic field quenching of the drift velocity, which exists at certain high magnetic fields in the absence of the THz radiation.

Acknowledgments

This work was supported by the National Natural Science Foundation of China (grant 60076011), the Ministry of Science and Technology of China, the Special Funds for Major State Basic Research Project (grant 2000683), the Shanghai Municipal Commission of Science and Technology, the Shanghai Foundation for Research and Development of Applied Materials, and the Shanghai Foundation for Research and Development of Applied Materials.

References

[1] Keay B J, Allen S J Jr, Galán J, Kaminski J P, Campman K L, Gossard A C, Bhattacharya U and Rodwell M J W 1995 *Phys. Rev. Lett.* **75** 4089
[2] Asmar N G, Markelz A G, Gwinn E G, Černe J, Sherwin M S, Campman K L, Hopkins P F and Gossard A C 1995 *Phys. Rev.* B **51** 18 041
[3] Unterrainer K, Keay B J, Wanke M C, Allen S J, Leonard D, Medeiros-Ribeiro G, Bhattacharya U and Rodwell M J W 1996 *Phys. Rev. Lett.* **76** 2973
[4] Schomburg E, Ignatov A A, Grenzer J, Renk K F, Pavel'ev D G, Koschurinov Yu, Melzer B Ja, Ivanov S, Schaposchnikov S and Kop'ev P S 1996 *Appl. Phys. Lett.* **68** 1096
[5] Ignatov A A, Schomburg E, Grenzer J, Renk K F and Dodin E P 1995 *Z. Phys.* B **98** 187
[6] Brandes T 1996 *Europhys. Lett.* **33** 629
[7] Lei X L, Dong B and Chen Y Q 1997 *Phys. Rev.* B **56** 12 120
[8] Xu W 1998 *Phys. Rev.* B **57** 12 939
Xu W 1998 *J. Phys.: Condens. Matter* **10** 6105
[9] Lei X L 1998 *J. Appl. Phys.* **84** 1396
Lei X L 1998 *J. Phys.: Condens. Matter* **10** 3201
[10] Liu S Y and Lei X L 1999 *Phys. Rev.* B **60** 10 624
[11] Bryskin V V and Kleinert P 1999 *Phys. Rev.* B **59** 8152
Kleinert P and Bryskin V V 1999 *J. Phys.: Condens. Matter* **11** 2539
[12] Shu W M and Lei X L 1994 *Phys. Rev.* B **50** 17 378
[13] Eaves L *et al* 1999 *Physica* B **272** 190
[14] Lei X L and Cui H L 1998 *Eur. Phys. J.* B **4** 513